Challenges in detecting topological superconducting transitions via supercurrent and phase probes in planar Josephson junctions

Pankaj Sharma and Narayan Mohanta
Department of Physics, Indian Institute of Technology Roorkee, Roorkee 247667, India

Topological superconductors harbor, at their boundaries and vortex cores, zero-energy Majorana bound states, which can be the building blocks in fault-tolerant topological quantum computing. Planar Josephson junctions host such topological superconducting phases, highly tunable by an external magnetic field or phase difference between the superconducting leads. Despite many theoretical and experimental studies, the signatures of the transition to a topological superconducting phase, based on minima in the critical supercurrent I_c flowing across the junction, the 0-π transition in the ground state junction phase and their anisotropic magnetic-field response have remained unsettled. Using rigorous numerical calculations with several experimentally relevant parameter settings, we show that I_c and φ_{GS} cannot indicate unambiguously a topological transition in any realistic planar junctions. Furthermore, the anisotropic variations of I_c and φ_{GS} with an in-plane magnetic field appear in junctions that are undoubtedly in a trivial superconducting phase, raising concerns on the effectiveness of these probes in identifying topological transitions in planar junctions. We discuss possible strategies to confirm a topological superconducting phase in these platforms.

I. INTRODUCTION

Conclusive identification of a topological superconducting phase hosting zero-energy Majorana bound states (MBS) is currently one of the central problems in condensed matter physics. The MBS, because of their non-Abelian statistics, are promising for building qubits for fault-tolerant topological quantum computing [1–5]. Extensive efforts in the past years in various geometries with strong Rashba spin-orbit coupling (RSOC), including semiconductor-superconductor nanowires [6–12], magnetic adatom-superconductor interfaces [13–17], topological insulator-superconductor interfaces [18–20], and oxide heterostructures [21,22], revealed a zero-bias conductance peak (ZBCP) signature to support the presence of the MBS. However, the challenge has been the disentanglement of the MBS from other low-energy quasiparticles, primarily Andreev bound states and impurity-induced states [23–32]. Therefore, to achieve the sought-after braiding of the MBS, and to overcome the inherent instabilities in one-dimensional nanowire networks, two-dimensional platforms such as the planar Josephson junctions were introduced [33–39].

A planar Josephson junction consists of a two-dimensional electron gas (2DEG), proximity coupled to two superconducting leads [shown schematically in Fig. 1(a)]. It has the additional advantage that the induced topological superconductivity can be easily controlled by the phase difference between the superconducting leads (tunable externally by applying a perpendicular magnetic field). The transition to a topological superconducting phase in these junctions, revealed by the emergence of the zero-energy MBS, appears at a critical value of an in-plane magnetic field, applied along the length of the nonsuperconducting channel when the phase difference between the superconducting leads is close to π

[34,40]. This topological superconducting transition has been suggested to be accompanied in general by a minimum in the critical supercurrent I_c and a jump from nearly 0 to nearly π in the ground state phase φ_{GS} [34]. Following this theoretical proposal, successive experiments reported the ZBCP signature of the MBS within a range of magnetic fields, predicted by the minima in I_c [41,42]. Further theoretical work suggested that for narrow superconducting leads ($W_{SC} \lesssim \xi$, where ξ is the superconducting coherence length), as used in the experiments, the minima in I_c do not necessarily indicate topological phase transitions [43]. However, a subsequent study, with joint experimental and theoretical efforts, concluded a π phase jump in the junction phase and a simultaneous minimum in I_c at a critical magnetic field to be a signature of a topological superconducting transition [44]. The conclusions were further supported by the evidence of anisotropic response of I_c and φ_{GS} with respect to the in-plane magnetic field. Despite intensive analyses to exclude possible nontopological origins, it remains unclear whether the correspondence between these critical fields can be generalized for different junction dimensions and realistic parameters such as RSOC strength. Moreover, these conflicting results created confusion regarding the viability of these quantities (I_c and φ_{GS}) as reliable indicators of a topological superconducting transition in these planar Josephson junctions.

In this paper, we show that the observables I_c, φ_{GS}, and their anisotropic magnetic-field response cannot predict a topological superconducting transition in any realistic planar Josephson junction, irrespective of $W_{SC} \lesssim \xi$ or $W_{SC} > \xi$. We confirm these findings using the presence (absence) of the zero-energy MBS as the direct indicator of the topological (trivial) phase, in our numerical calculations which were performed using various experimentally relevant parameter
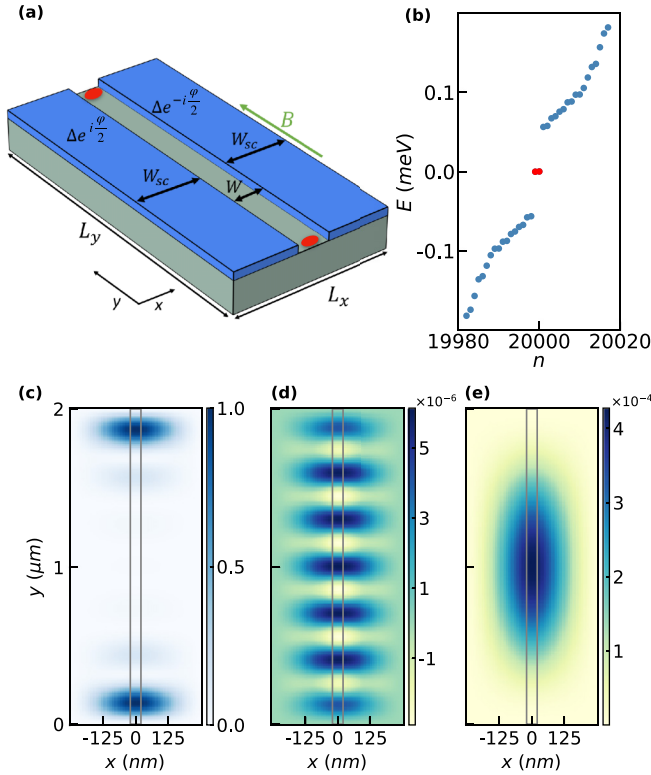
(a)

(b)

(c) **(d)** **(e)**

FIG. 1. (a) A schematic of the planar Josephson junction, created by placing two superconducting leads on top of a 2DEG based on a semiconducting quantum well. Red markers show the regions in the metallic channel where MBS are localized in the topological phase. (b) Energy eigenvalues vs their index n at $B = 1.5$ T, $\varphi = \pi$, and $\mu = -0.4$ meV, showing two eigenvalues at zero energy (in red), protected from the other states by an energy gap. (c) Local density of states profile (normalized) for the lowest positive energy eigenstate, revealing the localization of the two MBS at the ends of the metallic channel (shown by the gray lines). (d), (e) Profiles of charge density of states at $B = 1.5$ T (MBS present) and at $B = 0.5$ T (MBS absent), showing partial charge neutrality in the presence of MBS [color-bar scales show two orders of magnitude reduction in the charge density in (d)]. The junction parameters are $L_x = 0.5$ μm, $L_y = 2$ μm, and $W = 0.04$ μm.

settings and device geometries. Under realistic conditions, φ_{GS} exhibits a smooth monotonic variation with an in-plane magnetic field rather than a sharp jump. Even though the critical fields for the minima in I_c may coincidentally match with the critical field for the topological superconducting transition, we could not establish a general correspondence between the two critical fields. We also find that the anisotropy in I_c and φ_{GS} with respect to the in-plane magnetic field cannot conclusively distinguish a topological superconducting phase from a trivial one. We discuss a possible braiding realization of MBS as a prerequisite to conclude topological superconductivity in a multiterminal planar junction.

II. THEORETICAL MODEL

The planar Josephson junction devices used in the experiments [41,42,44] are made of a 2DEG, created at an

InAs/HgTe quantum well, and Al superconducting leads. To describe such a 2DEG with proximity-induced superconductivity underneath the superconducting leads, we use the Hamiltonian below,

$$
\mathcal{H} = \sum_{i,\sigma}(4t - \mu)c_{i\sigma}^{\dagger}c_{i\sigma} - t\sum_{\langle ij\rangle,\sigma}(c_{i\sigma}^{\dagger}c_{j\sigma} + \text{H.c.})
$$
$$
+ \sum_{i}(\Delta_i c_{i\uparrow}^{\dagger}c_{i\downarrow}^{\dagger} + \text{H.c.}) - \frac{g^*\mu_B B}{2}\sum_{i,\sigma,\sigma'}(\sigma_y)_{\sigma\sigma'}c_{i\sigma}^{\dagger}c_{i\sigma'}
$$
$$
- \frac{\mathbf{i}\alpha}{2a}\sum_{\langle ij\rangle,\sigma\sigma'}(\boldsymbol{\sigma}\times\mathbf{d}_{ij})_{\sigma\sigma'}^z c_{i\sigma}^{\dagger}c_{j\sigma'}, \tag{1}
$$

where $t = \hbar^2/2m^*a^2$ is the hopping energy, m^* is the effective mass of the electrons, a is unit spacing of the considered square lattice grid, i and j represent lattice site indices, σ and σ' are indices for spins ($\uparrow, \downarrow$), μ is the chemical potential, Δ_i is the superconducting pairing (conventional s wave) amplitude at site i, μ_B is the Bohr magneton, g^* is the effective g factor of the electrons, B is the magnetic field applied along the length of the metallic channel [y direction, in the chosen axes description, as shown in Fig. 1(a)], $\boldsymbol{\sigma}$ represents the Pauli matrices, α is the RSOC strength, $\mathbf{i}$ is the imaginary number, and $\mathbf{d}_{ij}$ denotes the unit vector from site i to j. The pairing amplitude is zero in the metallic channel and of constant magnitude on the two superconducting regions, but it has a phase difference of φ between the superconducting regions. We use open boundary conditions and the following parameters, $m^* = 0.026m_0$ (m_0 being the rest mass of electrons), $g^* = 10$, $\Delta = 0.2$ meV, and $\alpha = 30$ meV nm, typical for Al/InAs systems [45–47]. We use the lattice grid spacing $a = 10$ nm in our calculations throughout. The eigenvalues and eigenvectors of the Hamiltonian (1) were obtained by diagonalizing it using the unitary transformation $c_{i\sigma} = \sum_n u_{i\sigma}^n \gamma_n + v_{i\sigma}^{n*}\gamma_n^{\dagger}$, where $u_{i\sigma}^n$ ($v_{i\sigma}^n$) represents quasiparticle (quasihole) amplitudes, and γ_n ($\gamma_n^{\dagger}$) represents the fermionic annihilation (creation) operator of the Bogoliubov–de Gennes quasiparticles corresponding to the nth eigenstate.

III. RESULTS

A. Appearance of MBS

Zero-energy MBS appear at the two ends of the middle metallic channel of the planar Josephson junction when the phase difference φ between the superconducting leads is nearly π, and the length of the channel L_y is sufficiently large, so that the overlap between the two MBS appearing at its ends is minimized. Other essential requirements are (i) the RSOC strength needs to be greater than a critical value, which we found to be nearly 20 meV nm, and (ii) the magnetic-field strength B and chemical potential μ need to be chosen suitably within a range. The quasiparticle energy spectrum for our considered geometry ($L_y = 2$ μm, transverse length $L_x = 0.5$ μm, channel width $W = 0.04$ μm, and superconducting lead width $W_{SC} = 230$ nm [less than the coherence length $\xi = \hbar v_F/(\pi\Delta) \simeq 885$ nm]), shown in Fig. 1(b), reveals the presence of a pair of topologically protected zero-energy MBS at $\varphi = \pi$, $B = 1.5$ T, and $\mu = -0.4$ meV. These
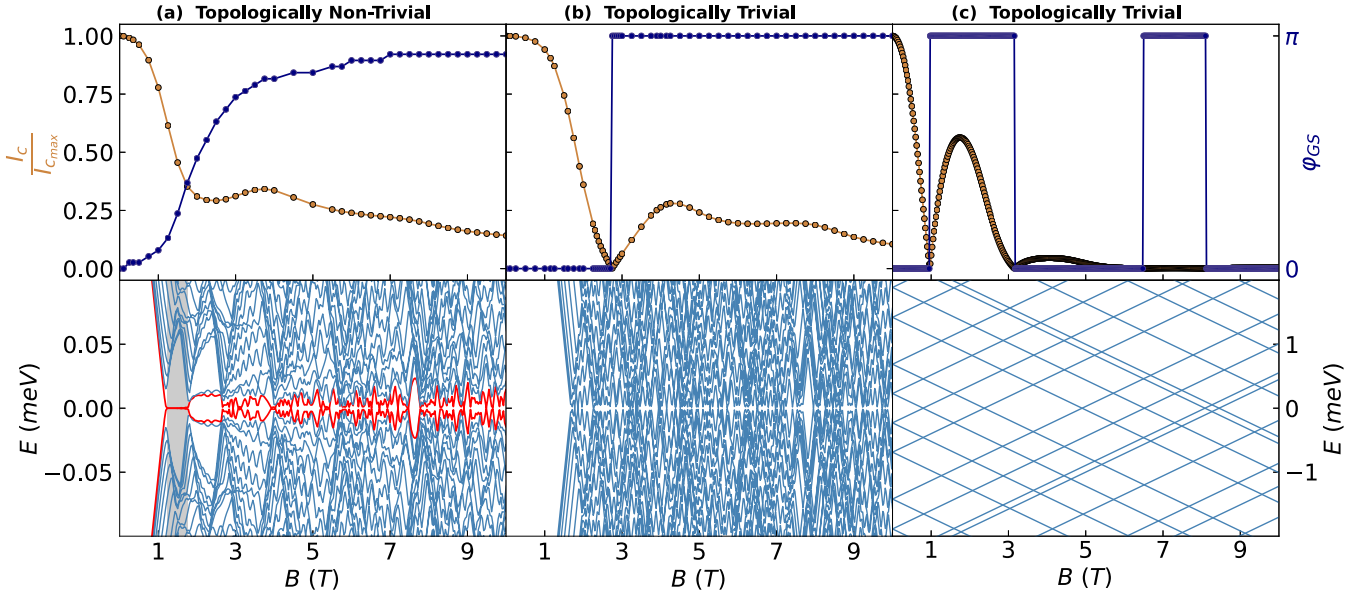
FIG. 2. Variation with the applied magnetic field B of the critical supercurrent I_c (normalized) and the ground state phase φ_{GS} (top row) and quasiparticle energy spectrum (bottom row) for three different cases: (a) a long planar Josephson junction ($L_x = 0.5\,\mu$m, $L_y = 2\,\mu$m, and $W = 0.04\,\mu$m) with RSOC strength $\alpha = 30$ meV nm, (b) the same junction as in (a) but with $\alpha = 0$, and (c) a relatively shorter junction ($L_x = 0.3\,\mu$m, $L_y = 0.15\,\mu$m, and $W = 0.1\,\mu$m) with $\alpha = 0$. The chemical potential in (a) and (b) is $\mu = -0.4$ meV and that in (c) is $\mu = 0.5$ meV; the phase difference between the superconducting leads in all three cases is $\varphi = \pi$. MBS do not appear in the quasiparticle energy spectra in (b) and (c), but I_c exhibits zeros at some critical fields and simultaneously sharp transitions in φ_{GS}. In case (a), MBS appear (shown by the red lines near zero energy within the grayed range of B), I_c shows a minimum at around $B = 2.5$ T, and φ_{GS} increases gradually from zero toward π with increasing B; however, the critical field for the minimum in I_c is different from the critical field at which MBS emerge.

zero-energy states are localized near the metallic channel ends, as shown by the local density of states profile in Fig. 1(c), obtained via $\rho_i = \sum_\sigma (|u_{i\sigma}|^2 + |v_{i\sigma}|^2)$ for the lowest positive-energy eigenstate. The local charge density of states $\rho_{ci} = \sum_\sigma (|u_{i\sigma}|^2 - |v_{i\sigma}|^2)$, at two magnetic fields, $B = 1.5$ T (with MBS) and $B = 0.5$ T (without MBS) as shown in Figs. 1(d) and 1(e), respectively, reveals a two orders-of-magnitude reduction in its value, indicating the realization of a partial charge neutrality, supporting further the appearance of the charge-neutral MBS in the junction. The charge density profile in the presence of MBS shows a density-wave-like pattern, a feature that generically appears in all geometries including the nanowire and planar Josephson junction ones, and is a manifestation of oscillatory MBS wave functions [48,49]. We use these direct confirmations of MBS to identify topological superconducting phase in our geometries.

B. Critical supercurrent and ground state phase

The observables of our main interest are the critical supercurrent I_c and the ground state phase φ_{GS}, which were predicted to be natural diagnostics for topological transitions in these Josephson junctions [34]. We calculate the critical supercurrent using $I_c = \max\{I(\varphi)\}$, where the supercurrent as a function of the phase difference φ is given by the thermodynamic relation [51,52]

$$I(\varphi) = \frac{2e}{\hbar}\frac{d\mathcal{F}}{d\varphi}, \qquad (2)$$

and the free energy $\mathcal{F}$ of the junctions is computed using quasiparticle energies E_n using the relation

$$\mathcal{F} = -2k_B T \sum_{E_n>0} \ln\left[2\cosh\left(\frac{E_n}{2k_B T}\right)\right], \qquad (3)$$

where k_B is the Boltzmann constant and T is the temperature. We use $k_B T = 0.43\Delta$ for the results presented here and explore the temperature effect in the Supplemental Material [50]. The ground state phase φ_{GS} is determined as the phase difference that minimizes $\mathcal{F}$. We obtain φ_{GS} within 0 and π, by mapping values appearing above π to this range.

In Fig. 2(a) (top panel), we show field variations of I_c and φ_{GS} for a long junction of dimension and parameters (with finite RSOC) as in Fig. 1. We find that I_c exhibits a minimum at $B \approx 4$ T, accompanied by a gradual increase in φ_{GS} from 0 toward π with increasing magnetic field strength B. The field variation of the quasiparticle energy spectrum [the bottom panel in Fig. 2(a)] reveals the emergence of zero-energy MBS within the range 1.1 T $\lesssim B \lesssim$ 1.7 T. Evidently, beyond $B \approx 2.5$ T, the junction is not in a topological superconducting phase since MBS are absent. The critical magnetic field $B \approx 2.5$ T, given by the first minimum in I_c, is therefore not consistent with the topological phase boundaries. On the other hand, φ_{GS} does not reveal any sharp transitions in this case with typical RSOC strengths, available in the discussed 2DEGs, and hence it is also not a good indicator for topological superconducting transitions. Figure 2(b) depicts a B variation of I_c, φ_{GS} (top panel), and of quasiparticle energy spectrum (bottom panel) for the same Josephson junction as in Fig. 2(a) but with
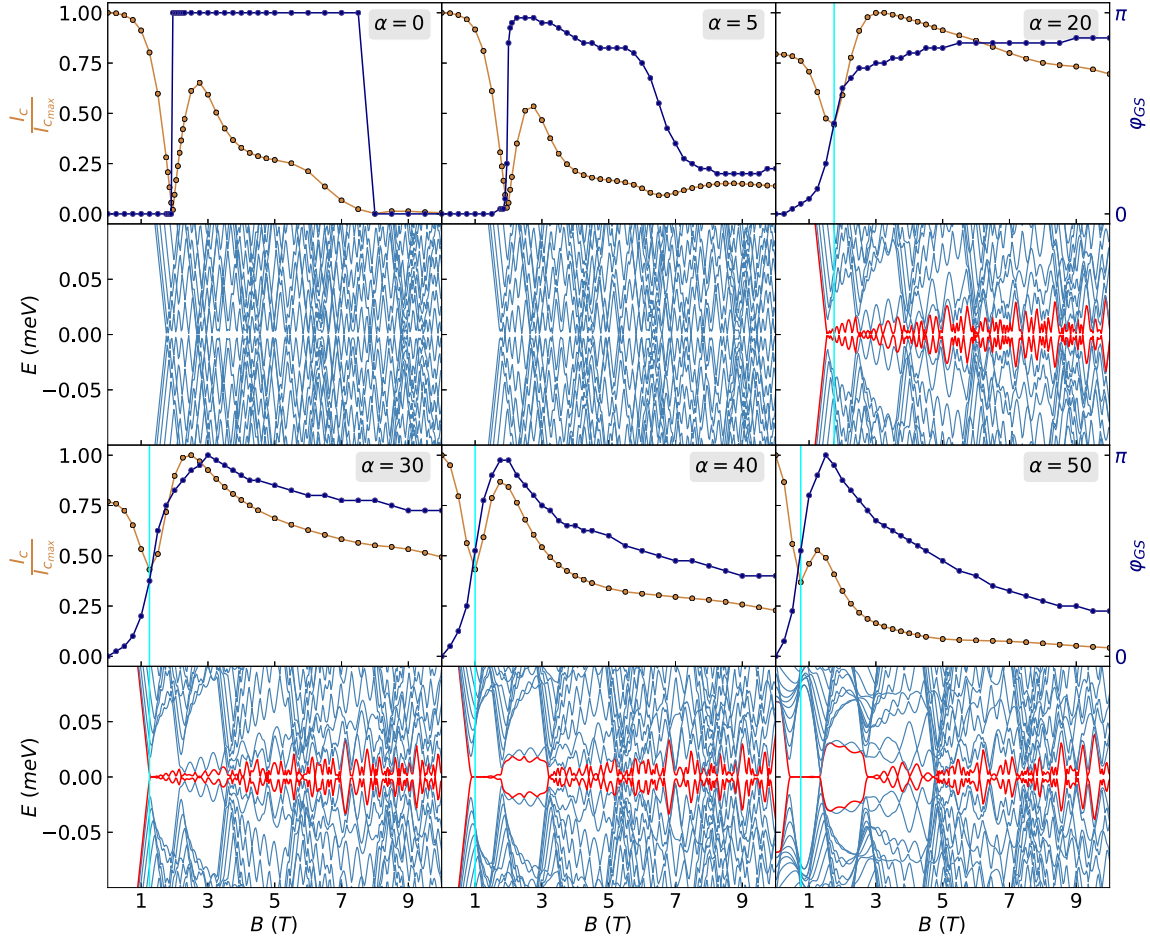
FIG. 3. Magnetic-field variation of critical supercurrent I_c (normalized) and ground state phase φ_{GS} (first and third rows), and corresponding quasiparticle energy spectrum (second and fourth rows) of a planar Josephson junction of dimension $L_x = 0.4\,\mu$m, $L_y = 1.6\,\mu$m, and $W = 0.08\,\mu$m, at different RSOC strengths α (in units of meV nm). Other parameters used are $\varphi = \pi$ and $\mu = -0.4$ meV. The cyan vertical lines show quantitative agreement of the critical field for the first minimum in I_c with the critical field for the emergence of zero-energy MBS.

zero RSOC. In this case, I_c exhibits a zero and φ_{GS} exhibits a sharp jump from 0 to π at a critical field $B \approx 2.75$ T; however, the junction is in a trivial phase since MBS do not appear for the entire range of B considered here. We confirm our findings by calculating I_c and φ_{GS} also for relatively shorter junctions; the results for a short junction of dimension $L_x = 0.3\,\mu$m, $L_y = 0.15\,\mu$m, and $W = 0.1\,\mu$m at zero RSOC are shown in Fig. 2(c). Multiple ranges of B, defined by $\varphi_{GS} \approx \pi$, can be identified clearly in this case, while the junction remains in a trivial superconducting phase. Because of the mean-field nature of the adopted formalism and constant pairing gap Δ, the critical fields are overestimated, i.e., larger than the actual critical fields found in experiments.

To explore the role of RSOC and variation in the width of the metallic channel in the agreement of the critical fields, we perform similar analyses at different RSOC strengths for a junction with a relatively wider metallic channel (dimension $L_x = 0.4\,\mu$m, $L_y = 1.6\,\mu$m, $W = 0.08\,\mu$m, and $W_{SC} = 160$ nm $< \xi$). From the results, shown in Fig. 3, we note the following: (i) I_c at the first minimum and at the first maximum increases with increasing RSOC strength α until $\alpha \approx 30$ meV nm, above which it decreases again; such a nonmonotonic field dependence exists also for shorter junctions [50]; (ii) sharp

transitions in φ_{GS} appear only for small values of α for which the Josephson junction is in a trivial phase always; the gradual increase in φ_{GS} with B was also found in Ref. [44]; and (iii) the second critical field for the second minimum of I_c or drop in φ_{GS} increases with increasing α. Therefore, for typical α values, available in the discussed 2DEGs, the second critical field will be beyond the usually realizable values. The near-zero-energy MBS start to appear above $\alpha \approx 20$ meV nm with a well-defined energy gap, and the critical field for the first minimum in I_c appears *near* the critical field for the topological superconducting transition. Coincidentally, the critical fields are in better agreement for the case of $\alpha = 30$ meV nm for this junction than the result presented in Fig. 2(a) for a junction with a narrower metallic channel. This comparison indicates that the agreement is better for junctions with a wider metallic region. However, there is no general correspondence among these critical fields, particularly for the long junctions considered in the experiments [41,42,44]. With increasing α, the critical field for the emergence of MBS decreases, compatible with RSOC-driven topological superconducting transitions.

We also investigate the in-plane magnetic field anisotropy in I_c, a signature used in Ref. [44] in support of the topological phase transition. We rotate the in-plane magnetic field angle θ
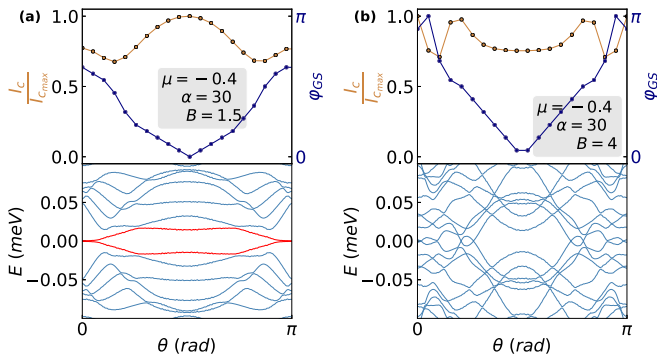
FIG. 4. Variation of I_c, φ_{GS}, and the quasiparticle energy spectrum with in-plane magnetic field angle θ at $\varphi = \pi$ (μ in units of meV, α in units of meV nm, and B in T) for two cases: (a) a topological phase at $\theta = 0$, and (b) a nontopological phase at $\theta = 0$. The system's dimensions are the same as in Fig. 3. Parameters are shown in the insets of the top panels.

(measured with respect to the $+y$ direction, along the length of the channel) from $\theta = 0$ to $\theta = \pi$, and plot I_c, φ_{GS}, and the energy spectrum in Fig. 4. We show two cases: (a) $B = 1.5$ T (a topological phase at $\theta = 0$ as shown in Fig. 3) and (b) $B = 4$ T (a nontopological phase at $\theta = 0$ as shown in Fig. 3), at a fixed RSOC strength $\alpha = 30$ meV nm. It is evident that the magnetic anisotropy in I_c and φ_{GS} exists in both cases. There is no noticeable difference in the field variation of I_c and φ_{GS} (see also Fig. S3 in Supplemental Material [50]). Hence, further evidence such as a demonstration of the non-Abelian characters of the MBS is required, in addition to the signatures in I_c and φ_{GS}, in order to unambiguously detect a topological superconducting transition in these planar junctions.

IV. DISCUSSION AND OUTLOOK

To generalize our findings, we performed similar calculations of I_c and φ_{GS}, as presented above for various other scenarios: (i) planar junctions with wider superconducting leads, i.e., $W_{SC} > \xi$ and wider channels, (ii) a magnetic field applied only in the metallic channel region, and (iii) a nonuniform g factor [50]. Based on these extensive analyses of different parameters and device geometries, we conclude that,

with realizable device dimensions and realistic parameters, I_c and φ_{GS} cannot identify topological superconducting transitions in planar Josephson junctions.

Other observables used in previous experiments include (i) the fractional ac Josephson effect and missing Shapiro steps due to the 4π periodic current-phase relation [53–58], (ii) the ZBCP signature [41,42,59,60], (iii) the bulk gap closing signature [59,60], (iv) local and nonlocal transport spectroscopy [59], and (v) negative conductance curvature at zero bias $(\partial^2 G/\partial V^2)|_{V=0}$ [42]. These signatures likely cannot confirm topological superconductivity separately due to the presence of non-Majorana states [61,62], but together may constitute a procedure for the detection of the topological superconductivity.

To look forward, it is intuitively appealing to explore more complicated geometries such as multiterminal planar Josephson junctions [63,64] for realizing Majorana fusion and non-Abelian Majorana braiding [40,65–69]. These complicated geometries may come with new challenges, one of them clearly being the issue of fixing the direction of the in-plane magnetic field which is required to be along the metallic channel length. This particular problem can be overcome by placing underneath the Josephson junction a chiral magnetic texture such as a skyrmion crystal which can provide a gauge field and create a two-dimensional topological superconductivity in the entire 2DEG [48,70]. Nonetheless, these planar Josephson junctions provide a versatile two-dimensional platform, capable of manipulating MBS with more efficient control knobs [71–75], and it is possible to realize even more exotic states [76,77].

[1] A. Kitaev, Unpaired Majorana fermions in quantum wires, Phys. Usp. **44**, 131 (2001).

[2] A.Y. Kitaev, Fault-tolerant quantum computation by anyons, Ann. Phys. **303**, 2 (2003).

[3] C. Nayak, S. H. Simon, A. Stern, M. Freedman, and S. Das Sarma, Non-Abelian anyons and topological quantum computation, Rev. Mod. Phys. **80**, 1083 (2008).

[4] J. Alicea, Y. Oreg, G. Refael, F. von Oppen, and M. P. A. Fisher, Non-Abelian statistics and topological quantum information processing in 1D wire networks, Nat. Phys. **7**, 412 (2011).

[5] J. Alicea, New directions in the pursuit of Majorana fermions in solid state systems, Rep. Prog. Phys. **75**, 076501 (2012).

[6] J. D. Sau, R. M. Lutchyn, S. Tewari, and S. Das Sarma, Generic new platform for topological quantum computation using semiconductor heterostructures, Phys. Rev. Lett. **104**, 040502 (2010).

[7] Y. Oreg, G. Refael, and F. von Oppen, Helical liquids and Majorana bound states in quantum wires, Phys. Rev. Lett. **105**, 177002 (2010).

[8] R. M. Lutchyn, J. D. Sau, and S. Das Sarma, Majorana fermions and a topological phase transition in semiconductor-superconductor heterostructures, Phys. Rev. Lett. **105**, 077001 (2010).

[9] V. Mourik, K. Zuo, S. M. Frolov, S. R. Plissard, E. P. A. M. Bakkers, and L. P. Kouwenhoven, Signatures of Majorana

fermions in hybrid superconductor-semiconductor nanowire devices, Science **336**, 1003 (2012).

[10] A. Das, Y. Ronen, Y. Most, Y. Oreg, M. Heiblum, and H. Shtrikman, Zero-bias peaks and splitting in an Al–InAs nanowire topological superconductor as a signature of Majorana fermions, Nat. Phys. **8**, 887 (2012).

[11] M. T. Deng, S. Vaitiekínas, E. B. Hansen, J. Danon, M. Leijnse, K. Flensberg, J. Nygård, P. Krogstrup, and C. M. Marcus, Majorana bound state in a coupled quantum-dot hybrid-nanowire system, Science **354**, 1557 (2016).

[12] F. Nichele, A. C. C. Drachmann, A. M. Whiticar, E. C. T. O'Farrell, H. J. Suominen, A. Fornieri, T. Wang, G. C. Gardner, C. Thomas, A. T. Hatke, P. Krogstrup, M. J. Manfra, K. Flensberg, and C. M. Marcus, Scaling of Majorana zero-bias conductance peaks, Phys. Rev. Lett. **119**, 136803 (2017).

[13] S. Nadj-Perge, I. K. Drozdov, B. A. Bernevig, and A. Yazdani, Proposal for realizing Majorana fermions in chains of magnetic atoms on a superconductor, Phys. Rev. B **88**, 020407(R) (2013).

[14] S. Nadj-Perge, I. K. Drozdov, J. Li, H. Chen, S. Jeon, J. Seo, A. H. MacDonald, B. A. Bernevig, and A. Yazdani, Observation of Majorana fermions in ferromagnetic atomic chains on a superconductor, Science **346**, 602 (2014).

[15] J. Li, T. Neupert, Z. Wang, A. H. MacDonald, A. Yazdani, and B. A. Bernevig, Two-dimensional chiral topological superconductivity in Shiba lattices, Nat. Commun. **7**, 12297 (2016).

[16] B. E. Feldman, M. T. Randeria, J. Li, S. Jeon, Y. Xie, Z. Wang, I. K. Drozdov, B. A. Bernevig, and A. Yazdani, High-resolution studies of the Majorana atomic chain platform, Nat. Phys. **13**, 286 (2017).

[17] N. Mohanta, A. P. Kampf, and T. Kopp, Supercurrent as a probe for topological superconductivity in magnetic adatom chains, Phys. Rev. B **97**, 214507 (2018).

[18] L. Fu and C. L. Kane, Superconducting proximity effect and Majorana fermions at the surface of a topological insulator, Phys. Rev. Lett. **100**, 096407 (2008).

[19] C.-K. Chiu, M. J. Gilbert, and T. L. Hughes, Vortex lines in topological insulator-superconductor heterostructures, Phys. Rev. B **84**, 144507 (2011).

[20] J.-P. Xu, M.-X. Wang, Z. L. Liu, J.-F. Ge, X. Yang, C. Liu, Z. A. Xu, D. Guan, C. L. Gao, D. Qian, Y. Liu, Q.-H. Wang, F.-C. Zhang, Q.-K. Xue, and J.-F. Jia, Experimental detection of a Majorana mode in the core of a magnetic vortex inside a topological insulator-superconductor Bi_2Te_3/$NbSe_2$ heterostructure, Phys. Rev. Lett. **114**, 017001 (2015).

[21] N. Mohanta and A. Taraphder, Topological superconductivity and Majorana bound states at the $LaAlO_3$/$SrTiO_3$ interface, Europhys. Lett. **108**, 60001 (2014).

[22] L. Kuerten, C. Richter, N. Mohanta, T. Kopp, A. Kampf, J. Mannhart, and H. Boschker, In-gap states in superconducting $LaAlO_3$/$SrTiO_3$ interfaces observed by tunneling spectroscopy, Phys. Rev. B **96**, 014513 (2017).

[23] G. Kells, D. Meidan, and P. W. Brouwer, Near-zero-energy end states in topologically trivial spin-orbit coupled superconducting nanowires with a smooth confinement, Phys. Rev. B **86**, 100503(R) (2012).

[24] E. Prada, P. San-Jose, and R. Aguado, Transport spectroscopy of NS nanowire junctions with Majorana fermions, Phys. Rev. B **86**, 180503(R) (2012).

[25] T. D. Stanescu, S. Tewari, J. D. Sau, and S. Das Sarma, To close or not to close: The fate of the superconducting gap across

the topological quantum phase transition in Majorana-carrying semiconductor nanowires, Phys. Rev. Lett. **109**, 266402 (2012).

[26] D. Rainis, L. Trifunovic, J. Klinovaja, and D. Loss, Towards a realistic transport modeling in a superconducting nanowire with Majorana fermions, Phys. Rev. B **87**, 024515 (2013).

[27] J. Cayao, E. Prada, P. San-Jose, and R. Aguado, SNS junctions in nanowires with spin-orbit coupling: Role of confinement and helicity on the subgap spectrum, Phys. Rev. B **91**, 024514 (2015).

[28] C.-X. Liu, J. D. Sau, T. D. Stanescu, and S. Das Sarma, Andreev bound states versus Majorana bound states in quantum dot-nanowire-superconductor hybrid structures: Trivial versus topological zero-bias conductance peaks, Phys. Rev. B **96**, 075161 (2017).

[29] H. J. Suominen, M. Kjaergaard, A. R. Hamilton, J. Shabani, C. J. Palmstrøm, C. M. Marcus, and F. Nichele, Zero-energy modes from coalescing Andreev states in a two-dimensional semiconductor-superconductor hybrid platform, Phys. Rev. Lett. **119**, 176805 (2017).

[30] A. Vuik, B. Nijholt, A. R. Akhmerov, and M. Wimmer, Reproducing topological properties with quasi-Majorana states, SciPost Phys. **7**, 061 (2019).

[31] H. Pan and S. Das Sarma, Physical mechanisms for zero-bias conductance peaks in Majorana nanowires, Phys. Rev. Res. **2**, 013377 (2020).

[32] S. Das Sarma and H. Pan, Disorder-induced zero-bias peaks in Majorana nanowires, Phys. Rev. B **103**, 195158 (2021).

[33] M. Hell, M. Leijnse, and K. Flensberg, Two-dimensional platform for networks of Majorana bound states, Phys. Rev. Lett. **118**, 107701 (2017).

[34] F. Pientka, A. Keselman, E. Berg, A. Yacoby, A. Stern, and B. I. Halperin, Topological superconductivity in a planar Josephson junction, Phys. Rev. X **7**, 021032 (2017).

[35] J. Shabani, M. Kjaergaard, H. J. Suominen, Y. Kim, F. Nichele, K. Pakrouski, T. Stankevic, R. M. Lutchyn, P. Krogstrup, R. Feidenhans'l, S. Kraemer, C. Nayak, M. Troyer, C. M. Marcus, and C. J. Palmstrøm, Two-dimensional epitaxial superconductor-semiconductor heterostructures: A platform for topological superconducting networks, Phys. Rev. B **93**, 155402 (2016).

[36] F. Nichele, E. Portolés, A. Fornieri, A. M. Whiticar, A. C. C. Drachmann, S. Gronin, T. Wang, G. C. Gardner, C. Thomas, A. T. Hatke, M. J. Manfra, and C. M. Marcus, Relating Andreev bound states and supercurrents in hybrid Josephson junctions, Phys. Rev. Lett. **124**, 226801 (2020).

[37] B. H. Wu, S. A. Hassan, X. F. Xu, C. R. Wang, W. J. Gong, and J. C. Cao, Quantum transport of planar Josephson junctions with Majorana bound states, Phys. Rev. B **102**, 085414 (2020).

[38] M. Alidoust, C. Shen, and Igor Žutić, Cubic spin-orbit coupling and anomalous Josephson effect in planar junctions, Phys. Rev. B **103**, L060503 (2021).

[39] D. Oshima, S. Ikegaya, A. P. Schnyder, and Y. Tanaka, Flat-band Majorana bound states in topological Josephson junctions, Phys. Rev. Res. **4**, L022051 (2022).

[40] M. Hell, K. Flensberg, and M. Leijnse, Coupling and braiding Majorana bound states in networks defined in two-dimensional electron gases with proximity-induced superconductivity, Phys. Rev. B **96**, 035444 (2017).

[41] H. Ren, F. Pientka, S. Hart, A. T. Pierce, M. Kosowsky, L. Lunczer, R. Schlereth, B. Scharf, E. M. Hankiewicz, L. W.

Molenkamp, B. I. Halperin, and A. Yacoby, Topological superconductivity in a phase-controlled Josephson junction, Nature (London) **569**, 93 (2019).

[42] A. Fornieri, A. M. Whiticar, F. Setiawan, E. Portolés, A. C. C. Drachmann, A. Keselman, S. Gronin, C. Thomas, T. Wang, R. Kallaher, G. C. Gardner, E. Berg, M. J. Manfra, A. Stern, C. M. Marcus, and F. Nichele, Evidence of topological superconductivity in planar Josephson junctions, Nature (London) **569**, 89 (2019).

[43] F. Setiawan, A. Stern, and E. Berg, Topological superconductivity in planar Josephson junctions: Narrowing down to the nanowire limit, Phys. Rev. B **99**, 220506(R) (2019).

[44] M. C. Dartiailh, W. Mayer, J. Yuan, K. S. Wickramasinghe, A. Matos-Abiague, I. Žutić, and J. Shabani, Phase signature of topological transition in Josephson junctions, Phys. Rev. Lett. **126**, 036802 (2021).

[45] T. P. Smith III and F. F. Fang, *g* factor of electrons in an InAs quantum well, Phys. Rev. B **35**, 7729 (1987).

[46] W. Mayer, J. Yuan, K. S. Wickramasinghe, T. Nguyen, M. C. Dartiailh, and J. Shabani, Superconducting proximity effect in epitaxial Al-InAs heterostructures, Appl. Phys. Lett. **114**, 103104 (2019).

[47] D. J. Carrad, M. Bjergfelt, T. Kanne, M. Aagesen, F. Krizek, E. M. Fiordaliso, E. Johnson, J. Nygård, and T. S. Jespersen, Shadow epitaxy for *in situ* growth of generic semiconductor/superconductor hybrids, Adv. Mater. **32**, 1908411 (2020).

[48] N. Mohanta, S. Okamoto, and E. Dagotto, Skyrmion control of Majorana states in planar Josephson junctions, Commun. Phys. **4**, 163 (2021).

[49] N. Mohanta, T. Zhou, J.-W. Xu, J. E. Han, A. D. Kent, J. Shabani, I. Žutić, and A. Matos-Abiague, Electrical control of Majorana bound states using magnetic stripes, Phys. Rev. Appl. **12**, 034048 (2019).

[50] See Supplemental Material at http://link.aps.org/supplemental/10.1103/PhysRevB.109.054515 for the supercurrent and phase signatures of planar Josephson junctions of different dimensions, and the effect of temperature on these probes.

[51] C. W. J. Beenakker, Three universal mesoscopic Josephson effects, in *Transport Phenomena in Mesoscopic Systems*, edited by H. Fukuyama and T. Ando, Springer Series in Solid-State Sciences Vol. 109 (Springer, Berlin, 1992), pp. 235–253.

[52] C. W. J. Beenakker and H. van Houten, The superconducting quantum point contact, in *Nanostructures and Mesoscopic Systems*, edited by W. P. Kirk and M. A. Reed (Academic Press, New York, 1992), pp. 481–497.

[53] H.-J. Kwon, K. Sengupta, and V. M. Yakovenko, Fractional ac Josephson effect in *p*- and *d*-wave superconductors, Eur. Phys. J. B **37**, 349 (2004).

[54] P. San-Jose, E. Prada, and R. Aguado, ac Josephson effect in finite-length nanowire junctions with Majorana modes, Phys. Rev. Lett. **108**, 257001 (2012).

[55] J. D. Sau and F. Setiawan, Detecting topological superconductivity using low-frequency doubled Shapiro steps, Phys. Rev. B **95**, 060501(R) (2017).

[56] L. P. Rokhinson, X. Liu, and J. K. Furdyna, The fractional a.c. Josephson effect in a semiconductor–superconductor nanowire as a signature of Majorana particles, Nat. Phys. **8**, 795 (2012).

[57] J. Wiedenmann, E. Bocquillon, R. S. Deacon, S. Hartinger, O. Herrmann, T. M. Klapwijk, L. Maier, C. Ames, C. Brüne, C. Gould, A. Oiwa, K. Ishibashi, S. Tarucha, H. Buhmann, and L. W. Molenkamp, 4π-periodic Josephson supercurrent in HgTe-based topological Josephson junctions, Nat. Commun. **7**, 10303 (2016).

[58] R. S. Deacon, J. Wiedenmann, E. Bocquillon, F. Domínguez, T. M. Klapwijk, P. Leubner, C. Brüne, E. M. Hankiewicz, S. Tarucha, K. Ishibashi, H. Buhmann, and L. W. Molenkamp, Josephson radiation from gapless Andreev bound states in HgTe-based topological Junctions, Phys. Rev. X **7**, 021011 (2017).

[59] A. Banerjee, O. Lesser, M. A. Rahman, C. Thomas, T. Wang, M. J. Manfra, E. Berg, Y. Oreg, A. Stern, and C. M. Marcus, Local and nonlocal transport spectroscopy in planar Josephson junctions, Phys. Rev. Lett. **130**, 096202 (2023).

[60] A. Banerjee, O. Lesser, M. A. Rahman, H.-R. Wang, M.-R. Li, A. Kringhøj, A. M. Whiticar, A. C. C. Drachmann, C. Thomas, T. Wang, M. J. Manfra, E. Berg, Y. Oreg, A. Stern, and C. M. Marcus, Signatures of a topological phase transition in a planar Josephson junction, Phys. Rev. B **107**, 245304 (2023).

[61] M. C. Dartiailh, J. J. Cuozzo, B. H. Elfeky, W. Mayer, J. Yuan, K. S. Wickramasinghe, E. Rossi, and J. Shabani, Missing Shapiro steps in topologically trivial Josephson junction on InAs quantum well, Nat. Commun. **12**, 78 (2021).

[62] D. Rosenbach, T. W. Schmitt, P. Schüffelgen, M. P. Stehno, C. Li, M. Schleenvoigt, A. R. Jalil, G. Mussler, E. Neumann, S. Trellenkamp, A. A. Golubov, A. Brinkman, D. Grützmacher, and T. Schäpers, Reappearance of first Shapiro step in narrow topological Josephson junctions, Sci. Adv. **7**, eabf1854 (2021).

[63] R.-P. Riwar, M. Houzet, J. S. Meyer, and Y. V. Nazarov, Multi-terminal Josephson junctions as topological matter, Nat. Commun. **7**, 11167 (2016).

[64] N. Pankratova, H. Lee, R. Kuzmin, K. Wickramasinghe, W. Mayer, J. Yuan, M. G. Vavilov, J. Shabani, and V. E. Manucharyan, Multiterminal Josephson effect, Phys. Rev. X **10**, 031051 (2020).

[65] K. Flensberg, Non-Abelian operations on Majorana fermions via single-charge control, Phys. Rev. Lett. **106**, 090503 (2011).

[66] B. van Heck, A. R. Akhmerov, F. Hassler, M. Burrello, and C. W. J. Beenakker, Coulomb-assisted braiding of Majorana fermions in a Josephson junction array, New J. Phys. **14**, 035019 (2012).

[67] T. Hyart, B. van Heck, I. C. Fulga, M. Burrello, A. R. Akhmerov, and C. W. J. Beenakker, Flux-controlled quantum computation with Majorana fermions, Phys. Rev. B **88**, 035121 (2013).

[68] A. Stern and E. Berg, Fractional Josephson vortices and braiding of Majorana zero modes in planar superconductor-semiconductor heterostructures, Phys. Rev. Lett. **122**, 107701 (2019).

[69] B. Pandey, N. Mohanta, and E. Dagotto, Out-of-equilibrium Majorana zero modes in interacting Kitaev chains, Phys. Rev. B **107**, L060304 (2023).

[70] M. M. Desjardins, L. C. Contamin, M. R. Delbecq, M. C. Dartiailh, L. E. Bruhat, T. Cubaynes, J. J. Viennot, F. Mallet, S. Rohart, A. Thiaville, A. Cottet, and T. Kontos, Synthetic spin–orbit interaction for Majorana devices, Nat. Mater. **18**, 1060 (2019).

[71] T. Laeven, B. Nijholt, M. Wimmer, and A. R. Akhmerov, Enhanced proximity effect in zigzag-shaped Majorana

Josephson junctions, Phys. Rev. Lett. **125**, 086802 (2020).

[72] M. Alidoust, M. Willatzen, and A.-P. Jauho, Strain-engineered Majorana zero energy modes and φ_0 Josephson state in black phosphorus, Phys. Rev. B **98**, 085414 (2018).

[73] B. Scharf, F. Pientka, H. Ren, A. Yacoby, and E. M. Hankiewicz, Tuning topological superconductivity in phase-controlled Josephson junctions with Rashba and Dresselhaus spin-orbit coupling, Phys. Rev. B **99**, 214503 (2019).

[74] C. M. Moehle, Chung T. Ke, Q. Wang, C. Thomas, D. Xiao, S. Karwal, M. Lodari, V. van de Kerkhof, R. Termaat, G. C. Gardner, G. Scappucci, M. J. Manfra, and S. Goswami, InSbAs two-dimensional electron gases as a platform for topological superconductivity, Nano Lett. **21**, 9990 (2021).

[75] P. P. Paudel, T. Cole, B. D. Woods, and T. D. Stanescu, Enhanced topological superconductivity in spatially modulated planar Josephson junctions, Phys. Rev. B **104**, 155428 (2021).

[76] J. Klinovaja and D. Loss, Time-reversal invariant parafermions in interacting Rashba nanowires, Phys. Rev. B **90**, 045118 (2014).

[77] Y. Vinkler-Aviv, P. W. Brouwer, and F. von Oppen, Z_4 parafermions in an interacting quantum spin Hall Josephson junction coupled to an impurity spin, Phys. Rev. B **96**, 195421 (2017).